J|A|C|S
ARTICLES
Published on Web 11/18/2006

Grafting and Patterned Grafting of Block Copolymer Nanotubes onto Inorganic Substrates

Kyoungmoo Koh,[†] Guojun Liu,*[,†] and C. Grant Willson[‡]

Contribution from the Department of Chemistry, Queen's University, 90 Bader Lane, Kingston, Ontario, Canada K7L 3N6, and the Department of Chemistry and Biochemistry, University of Texas at Austin, Austin, Texas 78712-1167

Received September 15, 2006; E-mail: guojun.liu@chem.queensu.ca

Abstract: Chemical patterning of inorganic substrates by soft lithography has enabled various high-tech applications and cutting-edge fundamental research. In this paper, we report on methods for the grafting and patterned grafting of block copolymer nanotubes onto glass and mica surfaces. Under optimized conditions the density of such grafted nanotubes can be high, and most of the grafted tubes are in a standing position even after solvent evaporation. Surfaces modified with exotic reagents such as block copolymer nanofibers or nanotubes may find applications in biosensing, etc.

I. Introduction

Chemical patterning of inorganic substrates using soft lithography has enabled various high-tech applications and cutting-edge fundamental research.[1−3] Chemically patterned surfaces have, for example, been used in controlling surface wettability,[4] in crystal engineering,[5] in minimizing biomolecule nonspecific adsorption,[6] in enabling biosensoring and high-throughput biomolecule analysis,[1] and in production of microlens arrays[7,8] and magnetic nanoparticle arrays.[9] Fundamental research enabled includes the controlled anchorage, i.e., the projection size and spatial arrangement control, of cells on surfaces and then the subsequent interrogation of properties of single cells and cell clusters.[1] While traditional reagents for chemical patterning of surfaces have many advantages, which include their ready availability, the patterning of surfaces with more exotic reagents such as block copolymer nanofibers[10−26] or nanotubes[27−34] may turn out to be more advantageous for certain applications such as directed cell growth[35] and the creation of superhydrophobic or superhydrophilic surfaces,[36,37] where surface roughness on the nanometer- and micrometer-scale is required.[38] Surfaces grafted with block copolymer nanotubes may lead also to new applications that have not been contemplated before. In this paper, we report on methods for grafting block copolymer nanotubes onto mica and glass substrates. Under optimized conditions the density of such grafted nanotubes can be high, and most of the grafted tubes are in a standing position even after solvent evaporation. It is further demonstrated that the nanotubes can be used to pattern surfaces chemically.

Preparation of the nanotubes used here has been reported before.[39,40] They were derived from polystyrene-*block*-poly(2-cinnamoyloxyethyl methacrylate)-*block*-poly(*tert*-butyl acrylate), PS-PCEMA-P*t*BA. The preparation involved casting films from

[†] Queen's University.
[‡] University of Texas at Austin.

(1) Whitesides, G. M.; Ostuni, E.; Takayama, S.; Jiang, X. Y.; Ingber, D. E. *Annu. Rev. Biomed. Eng.* **2001**, *3*, 335.
(2) Ozin, G. A.; Arsenault, A. C. *Nanochemistry: A Chemical Approach to Nanomaterials*; RSC Publishing: Cambridge, 2005.
(3) Ulman, A. *An Introduction to Ultrathin Organic Films - From Langmuir-Blodgett to Self-Assembly*; Academic Press: Boston, 1991.
(4) Abbott, N. L.; Folkers, J. P.; Whitesides, G. M. *Science* **1992**, *257*, 1380.
(5) Aizenberg, J.; Black, A. J.; Whitesides, G. M. *Nature* **1999**, *398*, 495.
(6) Prime, K. L.; Whitesides, G. M. *Science* **1991**, *252*, 1164.
(7) Wu, M. H.; Park, C.; Whitesides, G. M. *Langmuir* **2002**, *18*, 9312.
(8) Wu, M. H.; Whitesides, G. M. . *Micromech. Microeng.* **2002**, *12*, 747.
(9) Zhong, Z. Y.; Gates, B.; Xia, Y. N.; Qin, D. *Langmuir* **2000**, *16*, 10369.
(10) Liu, G. J.; Qiao, L. J.; Guo, A. *Macromolecules* **1996**, *29*, 5508.
(11) Liu, G. J.; Ding, J. F.; Qiao, L. J.; Guo, A.; Dymov, B. P.; Gleeson, J. T.; Hashimoto, T.; Saijo, K. *Chem. Eur. J.* **1999**, *5*, 2740.
(12) Liu, G. J.; Yan, X. H.; Qiu, X. P.; Li, Z. *Macromolecules* **2002**, *35*, 7742.
(13) Liu, G. J.; Yan, X. H.; Duncan, S. *Macromolecules* **2002**, *35*, 9788.
(14) Liu, G. J.; Yan, X. H.; Duncan, S. *Macromolecules* **2003**, *36*, 2049.
(15) Yan, X.; Liu, G.; Li, H. *Langmuir* **2004**, *20*, 4677.
(16) Won, Y. Y.; Davis, H. T.; Bates, F. S. *Science* **1999**, *283*, 960.
(17) Wang, X. S.; Arsenault, A.; Ozin, G. A.; Winnik, M. A.; Manners, I. *J. Am. Chem. Soc.* **2003**, *125*, 12686.
(18) Templin, M.; Franck, A.; DuChesne, A.; Leist, H.; Zhang, Y. M.; Ulrich, R.; Schadler, V.; Wiesner, U. *Science* **1997**, *278*, 1795.
(19) Bang, J.; Jain, S. M.; Li, Z. B.; Lodge, T. P.; Pedersen, J. S.; Kesselman, E.; Talmon, Y. *Macromolecules* **2006**, *39*, 1199.
(20) Ishizu, K.; Ikemoto, T.; Ichimura, A. *Polymer* **1999**, *40*, 3147.
(21) Ma, Q. G.; Remsen, E. E.; Clark, C. G.; Kowalewski, T.; Wooley, K. L. *Proc. Natl. Acad. Sci. U.S.A.* **2002**, *99*, 5058.
(22) Liu, Y. F.; Abetz, V.; Muller, A. H. E. *Macromolecules* **2003**, *36*, 7894.
(23) Dalhaimer, P.; Bermudez, H.; Discher, D. E. *J. Polym. Sci. B: Polym. Phys.* **2004**, *42*, 168.
(24) Dalhaimer, P.; Bates, F. S.; Discher, D. E. *Macromolecules* **2003**, *36*, 6873.
(25) Silva, G. A.; Czeisler, C.; Niece, K. L.; Beniash, E.; Harrington, D. A.; Kessler, J. A.; Stupp, S. I. *Science* **2004**, *303*, 1352.
(26) Zhang, L. F.; Eisenberg, A. *J. Am. Chem. Soc.* **1996**, *118*, 3168.
(27) Stewart, S.; Liu, G. *Angew. Chem. Int. Ed. Engl.* **2000**, *39*, 340.
(28) Yan, X. H.; Liu, F. T.; Li, Z.; Liu, G. J. *Macromolecules* **2001**, *34*, 9112.
(29) Yan, X. H.; Liu, G. J.; Liu, F. T.; Tang, B. Z.; Peng, H.; Pakhomov, A. B.; Wong, C. Y. *Angew. Chem. Int. Ed. Engl.* **2001**, *40*, 3593.
(30) Grumelard, J.; Taubert, A.; Meier, W. *Chem. Commun.* **2004**, 1462.
(31) Raez, J.; Manners, I.; Winnik, M. A. *J. Am. Chem. Soc.* **2002**, *124*, 10381.
(32) Yu, K.; Zhang, L. F.; Eisenberg, A. *Langmuir* **1996**, *12*, 5980.
(33) Jenekhe, S. A.; Chen, X. L. *Science* **1998**, *279*, 1903.
(34) Raez, J.; Barjovanu, R.; Massey, J. A.; Winnik, M. A.; Manners, I. *Angew. Chem. Int. Ed. Engl.* **2000**, *39*, 3862.
(35) Stupp, S. I. *MRS Bull.* **2005**, *30*, 546.
(36) Jin, M. H.; Feng, X. J.; Feng, L.; Sun, T. L.; Zhai, J.; Li, T. J.; Jiang, L. *Adv. Mater.* **2005**, *17*, 1977.
(37) Vogelaar, L.; Lammertink, R. G. H.; Wessling, M. *Langmuir* **2006**, *22*, 3125.
(38) Gao, L. C.; McCarthy, T. J. *Langmuir* **2006**, *22*, 2966.
(39) Liu, G.; Yan, X.; Li, Z.; Zhou, J.; Duncan, S. *J. Am. Chem. Soc.* **2003**, *125*, 14039.
(40) Yan, X.; Liu, G.; Li, Z. *J. Am. Chem. Soc.* **2004**, *126*, 10059.

10.1021/ja066684d CCC: $33.50

Scheme 1. Preparation of Amino-End-Functionalized and Fluorescein-Encapsulated Nanotubes

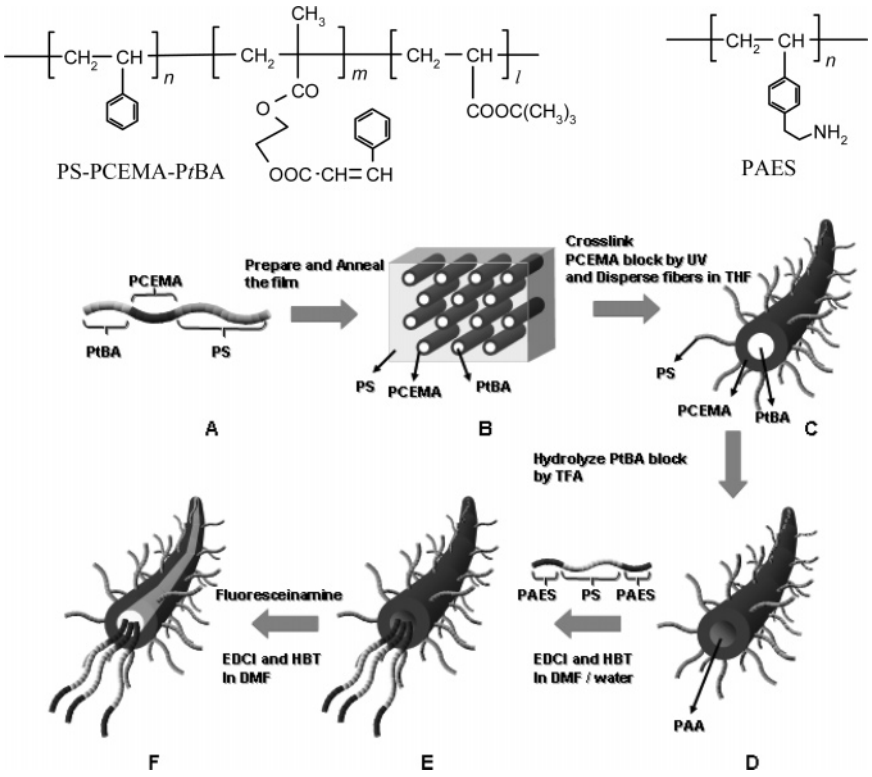

the triblock containing some PS homopolymer (A → B, Scheme 1). In such films, P*t*BA and PCEMA formed hexagonally packed concentric core−shell cylinders dispersed in the PS matrix.[41−43] The films were then irradiated to cross-link the PCEMA shell cylinders. PS-PCEMA-P*t*BA nanofibers were separated from one another or levitated out of the films by stirring such films in THF (B → C), which is a good solvent for PS, un-cross-linked PCEMA, and P*t*BA. They were shortened by ultrasonication to expose the core P*t*BA chains at the fiber ends. Nanotubes with poly(acrylic acid)- or PAA-lined cores were obtained after the hydrolysis of the *tert*-butyl groups from the P*t*BA cores (C → D). To introduce amino groups to the ends of the nanotubes, we reacted the end-exposed PAA chains with poly[4-(2-aminoethyl)styrene]-*block*-polystyrene-*block*-poly[4-(2-aminoethyl)styrene], PAES-PS-PAES (D → E). The PAA chains in the core of the nanotubes were reacted also with fluoresceinamine to make the nanofibers fluorescent for fluorescence microscopy studies (E → F).

To graft nanotubes, we started by introducing amino groups onto mica or glass surfaces by treating them with 3-aminopropyltrimethoxysilane (APTMS). The amino groups were reacted with succinic anhydride, suberic acid, or PAA to convert the amino groups to carboxyl groups. Nanotubes were attached via amidization between the amino terminal groups of the nanotubes and the surface carboxyl groups. To pattern the surfaces, we used a photolithographic process.[44] We started by spin-coating a thin layer of poly(2-cinnamoyloxyethyl acrylate), PCEA, on a glass or mica substrate. The surface was then irradiated using a TEM grid as the mask to cross-link PCEA in areas under exposure. Regions not exposed were freed of PCEA after solvent development and were functionalized by APTMS to introduce amino groups. Nanotubes were grafted onto areas containing amino groups using suberic acid as the connector yielding nanotube-patterned surfaces that are analogous to those decorated by metal nanorods.[45]

Aside from possible applications of grafted nanotubes in modifying surface properties, we envision potential applications of fluorescent block copolymer nanoposts as anchors for biomolecules in sensor devices and in immunoassays just as fluorescent metal nanorods do.[46,47] One can also imagine the use of these nanoposts with PS surfaces to direct the macroscopic alignment[48] along nanopost axial direction of cylindrical domains of PS-containing diblocks, where PS serves as the matrix block and the other block segregates to form cylinders. Like carbon nanotubes,[49] fluorescent water-dispersible nanotubes prior their grafting may be used in areas ranging from bioimaging to tissue engineering.

II. Results and Discussion

Polymer Characterization. The methodologies for the synthesis of PS-PCEMA-P*t*BA and PAES-PS-PAES of other compositions have been described before[39] and were, therefore, not repeated here. Homopolymer PCEA was derived from poly(2-hydroxyethyl acrylate) or PHEA. The precursor to PHEA

(41) Breiner, U.; Krappe, U.; Abetz, V.; Stadler, R. *Macromol. Chem. Phys.* **1997**, *198*, 1051.
(42) Bates, F. S.; Fredrickson, G. H. *Phys. Today* **1999**, *52*, 32.
(43) Park, C.; Yoon, J.; Thomas, E. L. *Polymer* **2003**, *44*, 6725.
(44) Thompson, L. F.; Willson, C. G.; Bowden, M. J., *Introduction to Microlithography*, 2nd ed.; American Chemical Society: Washington, DC, 1994.
(45) Kovtyukhova, N. I.; Mallouk, T. E. *Chem. Eur. J.* **2002**, *8*, 4355.
(46) Lee, K. B.; Park, S.; Mirkin, C. A. *Angew. Chem. Int. Ed. Engl.* **2004**, *43*, 3048.
(47) Nam, J. M.; Stoeva, S. I.; Mirkin, C. A. *J. Am. Chem. Soc.* **2004**, *126*, 5932.
(48) Thurn-Albrecht, T.; Schotter, J.; Kastle, C. A.; Emley, N.; Shibauchi, T.; Krusin-Elbaum, L.; Guarini, K.; Black, C. T.; Tuominen, M. T.; Russell, T. P. *Science* **2000**, *290*, 2126.
(49) Chen, X.; Tam, U. C.; Czlapinski, J. L.; Lee, G. S.; Rabuka, D.; Zettl, A.; Bertozzi, C. R. *J. Am. Chem. Soc.* **2006**, *128*, 6292.

Table 1. Characteristics of the Triblock Copolymers Used

sample	SEC M_w/M_n	dn_r/dc (mL/g)	LS $M_w \times 10^{-4}$ (g/mol)	NMR *n*/*m*/*l*	*n*	*m*	*l*
PS-PCEMA-P*t*BA	1.14	0.145	11.8	5.0/1.0/1.1	630	125	135
P(AES-TMS)-PS-P(AES-TMS)	1.21	0.193	2.3	1.0/41/1.0	5	200	5
PCEA	2.58	0.142	2.0		80		

was poly(trimethylsiloxyethyl acrylate) or P(HEA-TMS), which was prepared by free radical polymerization following procedures also reported before.[50] For characterization, the size exclusion chromatography (SEC) polydispersity indices M_w/M_n were measured in THF based on PS standards. The specific refractive index increments dn_r/dc and light scattering (LS) weight-average molar masses M_w were determined in THF for PS-PCEMA-P*t*BA and P(AES-TMS)-PS-P(AES-TMS), respectively, where P(AES-TMS) denotes poly{4-[2-*N*,*N*-bis(trimethylsilyl)aminoethyl]styrene}, a precursor to PAES. The ratios *n*/*m*/*l* between the numbers of repeat units for the PS, PCEMA, and P*t*BA blocks for the PS-PCEMA-P*t*BA triblock and *n*/*m*/*n* for P(AES-TMS)-PS-P(AES-TMS) were determined from ^{1}H nuclear magnetic resonance (NMR) analysis. Table 1 summarizes the characteristics of the samples used in this study. We have included the weight-average number of repeat units calculated using the LS M_w and NMR *n*/*m*/*l* or *n*/*m*/*n* values rather than the number-average number of repeat units for PS, PCEMA, P*t*BA, and P(AES-TMS) in the table because the SEC M_w/M_n values were inaccurate for the triblock.

Nanotubes with Grafted PAES-PS-PAES Terminal Chains. The preparation of PS-PCEMA-PAA nanotubes with grafted terminal PAES-PS-PAES chains has been reported by us before.[39] The process involved first film formation from PS-PCEMA-P*t*BA/PS. By adjusting the mass fraction between PS-PCEMA-P*t*BA and PS to 3.0/1.0, we obtained a total volume fraction of 32% for PCEMA and P*t*BA. The PCEMA and P*t*BA blocks in such films formed core−shell cylinders dispersed in the PS matrix. The PCEMA shell cylinders were then cross-linked by UV irradiation of the films and the cross-linked cylinders were separated from one another under vigorous stirring in THF to yield nanofibers. The nanofibers were subsequently cut short by ultrasonication to expose the core P*t*BA chains. Before use, the samples were purified by centrifugation precipitation.

Figure 1 shows a TEM image of the nanofibers that we used. Hemispherical end caps are not seen for most of the fibers suggesting the exposure of the P*t*BA core chains at the fiber termini. The average diameter of the fibers in the figure is 65 ± 7 nm. The weight- and number-average lengths of the relatively short fibers with their entire contours seen in Figure 1 are 540 and 370 nm, respectively.

Treating the nanofibers with trifluoroacetic acid led to the hydrolysis of P*t*BA to PAA, producing nanotubes with PAA-lined cores. Amino groups were grafted to the nanotube ends by reacting PAES-PS-PAES with the end-exposed PAA chains of the nanotubes. To estimate the number of PAES-PS-PAES chains, n_g, attached to each nanotube end we reacted the PAES amino groups with Rhodamine B following a method described before.[39] After sample purification, the Rhodamine B absorbance was determined and used in combination with the number-average TEM length, diameter, and the estimated molar mass of the nanotubes to evaluate n_g.[39] Assuming that each PAES-PS-PAES chain reacted with five Rhodamine B molecules we obtained a n_g value of ∼32. In reality, not all of the AES groups in the free PAES block could react with Rhodamine B. We believe that the n_g value should be higher.

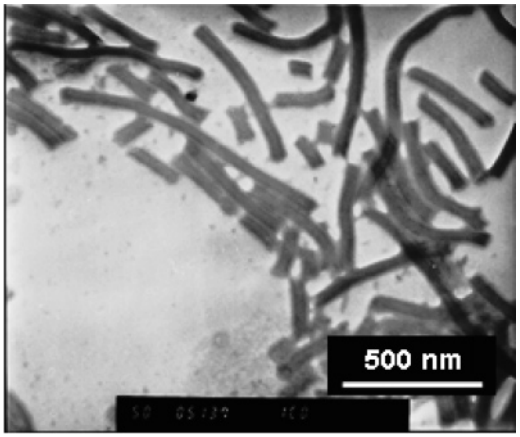

Figure 1. TEM images of nanofibers after ultrasonication and purification by centrifugation.

Fluorescein-Encapsulated Nanotubes. The residual AA groups in the core of the nanotubes were further reacted with fluoresceinamine again by amidization to introduce fluorophores. The covalent attachment of fluorescein to the nanotubes could be judged by the light yellow color that the nanotubes bore after reaction with fluoresceinamine and sample purification. Assuming that fluorescein groups inside the nanotube cores have the same extinction coefficient as fluoresceinamine, we determined quantitatively a fluoresceinamine labeling amount of 0.128 g per gram of nanotubes.

Surface Modification by APTMS. The APTMS treatment method has been practiced by many researchers to modify the surface of mica as sample support for atomic force microscopy applications[51] and its effectiveness is thus expected. We confirmed the effectiveness of this method from a water contact angle change before and after APTMS treatment of a surface. Before APTMS treatment, water spread well on a mica surface and we had difficulty in estimating such a small water contact angle. After APTMS treatment, the water contact angle θ_w increased to 46 ± 5° as shown in Figure 2. We did not determine the θ_w value on glass substrate after APTMS treatment as we expected the reactions to be similar and occur with comparable effectiveness. This assessment is confirmed by our ultimate success in grafting fluorescent nanotubes on glass surfaces as will be discussed later.

To gain more insight into the mechanism for water contact angle changes, we determined also the ethylene glycol contact angle θ_{EG} for an APTMS-treated mica surface and also θ_{EG} at

(50) Liu, G.; Yang, H.; Zhou, J.; Law, S. J.; Jiang, Q.; Yang, G. *Biomacromolecules* **2005**, *6*, 1280.

(51) Wang, H. D.; Bash, R.; Yodh, J. G.; Hager, G. L.; Lohr, D.; Lindsay, S. M. *Biophys. J.* **2002**, *83*, 3619.

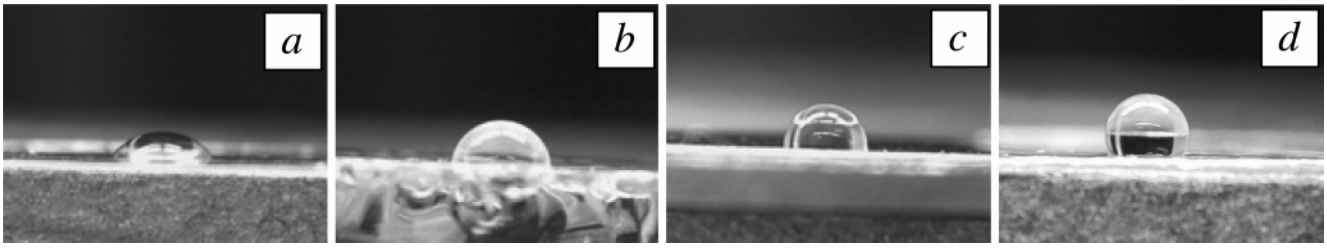

Figure 2. Photographs of water droplets on APTMS-modified mica (*a*), PS plate (*b*), mica grafted with nanotubes using succinic anhydride (*c*), and suberic acid (*d*) as the connector. The width of each picture frame corresponds to ~8 mm.

Table 2. Results of Surface Free Energy Measurements

sample	θ_W	θ_{EG}	γ_D (mJ/m^2)	γ_P (mJ/m^2)
APTMS-modified mica	46 ± 5	39 ± 2	45	44
mica after succinic anhydride treatment	19 ± 2	28 ± 1	51	70
mica after PAA treatment	44 ± 4	39 ± 2	44	47
nanotube-grafted mica using succinic anhydride as spacer	90 ± 1	55 ± 8	34	2.2
nanotube-grafted mica using PAA as spacer	68 ± 3	41 ± 2	44	15
nanotube-grafted mica using suberic acid as spacer	101 ± 4	51 ± 2	37	0.3
PS plate	82 ± 2	56 ± 4	34	8

different surface treatment stages with results shown in Table 2. The surface energy γ of a solid substrate can be normally broken into a dispersion component γ_D and a polar component γ_P. With the γ_D and γ_P values known for water and ethylene glycol and θ_W and θ_{EG} measured on a given solid substrate, we calculated γ_D and γ_P for the substrate following an equation proposed by Owen and Wendt.[52,53] These values are also listed in Table 2.

Reaction of APTMS-Modified Surfaces with Succinic Anhydride. We have previously successfully reacted succinic anhydride with hydroxyl groups of polymers to introduce carboxyl groups.[54,55] The amidization reaction should occur more readily than the esterification reaction between hydroxyl groups and succinic anhydride. To ensure a high degree of amino group conversion, a large excess of succinic anhydride was used. After reaction, the surfaces were rinsed with 0.1 M HCl to ensure that the resultant carboxyl groups are in the acidic form.

Occurrence of the above reaction was again supported by results of Table 2 from θ_W and θ_{EG} measurements. After the introduction of the carboxyl groups, the θ_W and θ_{EG} values decreased substantially. Application of the Owen and Wendt equation showed that the surfaces after succinic anhydride treatment became considerably more hydrophilic and polar as characterized by a large γ_P value.

Reaction of APTMS-Modified Surfaces with PAA. Amidization between amino and carboxyl groups is used to make polypeptides.[56] Amidization between the terminal amino groups of PS-PCEMA-PAA nanotubes and the carboxyl groups on the surfaces of water-soluble nanospheres has previously allowed us to prepare super-surfactant.[39] This reaction has also allowed us to couple nanotubes of different compositions to prepare block copolymer nanotube multiblocks.[40] Its effectiveness here in grafting the PAA chains to APTMS-modified surfaces was thus expected.

There were no changes, within experimental error, in the θ_W and θ_{EG} values in Table 2 before and after PAA chain grafting. Our literature search revealed that the θ_W value of PAA is 46°.[57] Thus, the insignificant changes in the θ_W and θ_{EG} values after PAA grafting was probably due to the accidental match between the surface properties of PAA and APTMS-modified mica surfaces. Furthermore, the PAA chains, possessing reduced conformational flexibility relative to small-molecule carboxyl groups, may not react with all of the surface amine groups. Despite no changes in θ_W and θ_{EG}, our success in grafting PAA will become self-evident later when we discuss the highly efficient attachment of amino-terminated nanotubes on to PAA-modified mica or glass substrates.

Nanotube Grafting on Succinic Anhydride and PAA Modified Mica Surfaces. Nanotubes bearing terminal amino groups were grafted to succinic anhydride- or PAA-modified mica or glass substrate again via amidization. Figure 3 shows AFM images of two regions of a mica sample grafted with nanotubes, where the mica plate was modified with succinic anhydride prior to nanotube grafting by soaking the plate in a nanotube solution at 0.2 wt % in *N*,*N*-dimethylforamide (DMF) containing *N*,*N*′-dicyclohexylcarbodimide (DCC) and HBT (1-hydroxybenzotriazole). The fact that the nanotubes were covalently attached to the mica surface was established from the following observations. First, they could not be rinsed off the substrate regardless of how many times we tried to rinse the samples with DMF. Second, we have repeated the nanotube grafting and DMF rinsing procedure under conditions otherwise identical to those utilized in a normal grafting experiment except the omitted DCC use. Such a control experiment showed a lack of nanotubes on mica surface after DMF rinsing.

The three-dimensional (3D) image in Figure 3 reveals that the grafted objects can be classified roughly into two categories. The relatively long tubes belong to category one. These tubes lie flat on the mica surface with a tube diameter of 46 ± 6 nm as estimated from the peak height of 21 such tubes. This value is smaller than 65 ± 7 nm determined from TEM for the PS-PCEMA-P*t*BA nanofibers of Figure 1, suggesting the flattening of the nanotubes on a substrate after solvent evaporation. The relatively short fibers belong to category two. They seem to stand vertically on the mica surfaces with height typically less than ~250 nm. The standing tubes are not perfectly cylindrical but assume the shape of an AFM tip because the tip was not

(52) Owens, D. K.; Wendt, R. C. *J. Appl. Polym. Sci.* **1969**, *13*, 1741.
(53) van Krevelen, D. W. *Properties of Polymers - Their Correlation with Chemical Structure; Their Numerical Estimation and Prediction from Additive Group Contributions*, 3rd ed.; Elsevier Science: Amsterdam, 1997.
(54) Li, Z.; Liu, G.; Law, S. J.; Sells, T. *Biomacromolecules* **2002**, *3*, 984.
(55) Zheng, R. H.; Liu, G. J.; Yan, X. H. *J. Am. Chem. Soc.* **2005**, *127*, 15358.
(56) Cui, L.; Tong, X.; Yan, X. H.; Liu, G. J.; Zhao, Y. *Macromolecules* **2004**, *37*, 7097.
(57) Lee, S. D.; Hsiue, G. H.; Chang, P. C. T.; Kao, C. Y. *Biomaterials* **1996**, *17*, 1599.

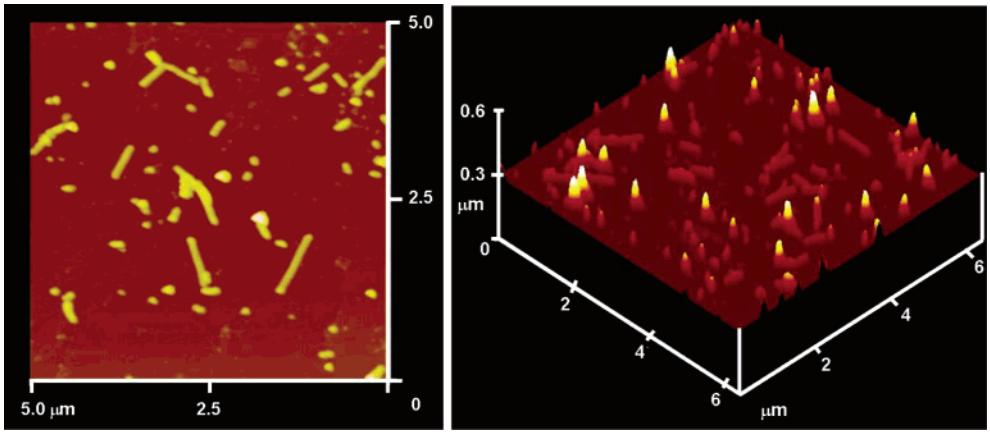

Figure 3. AFM images of nanotubes grafted on mica surface using succinic anhydride as the connector.

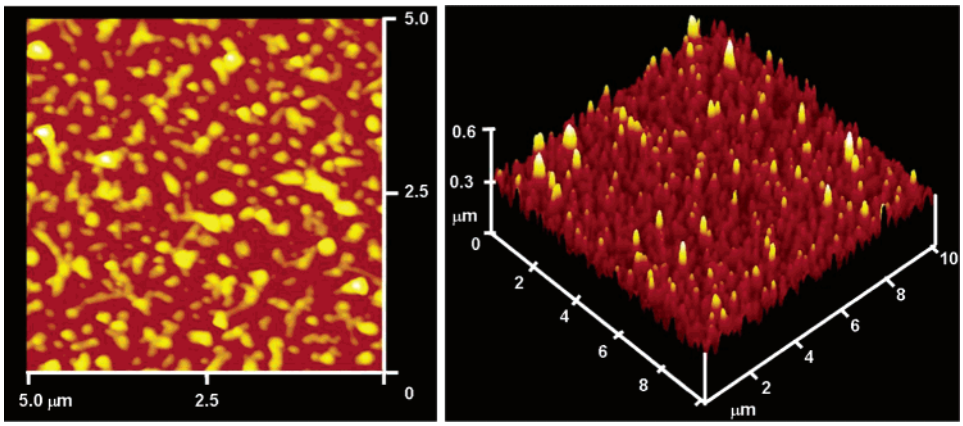

Figure 4. AFM images of nanotubes grafted on mica surface using PAA as the connector.

infinitely thin and was imaged by the standing nanotubes. The observation of many standing tubes suggests that the tubes were attached to the mica surfaces mainly via end grafting. The fact that the tubes remained standing despite the tapping force exerted by the oscillating AFM tip suggests that the tubes were grafted on the surface via multi PAE-PS-PAE chain attachment. The longer tubes could not retain their standing position after solvent evaporation probably because not all of the tubes were perfectly vertically grafted. At the same slanting angle, a longer tube produces a larger down or falling force on the connecting or hinging PAE-PS-PAE chains and is thus more likely to fall down after solvent evaporation. A tube does not stand perfectly vertically for potentially several reasons. A principal cause might be that the tubes were not cut by ultrasonication perfectly perpendicular to their axial direction.

While the figure clearly shows that we were successful in grafting the nanotubes, the grafting density is, however, rather low. We tried to increase the grafting density by increasing the nanotube solution concentration in DMF to 3.2 wt %. This did not increase the grafting density noticeably. This prompted us to suspect that the grafting density was limited by the accessibility of the carboxyl groups on the surface of a succinic anhydride modified mica plate. While the carboxyl group monolayer might be dense, such groups should be concentrated in a thin or essentially two-dimensional (2D) layer. Efficient reaction between such a monolayer and the PAES-PS-PAES chains attached to the end of a nanotube requires a PAES block to lie flat on the monolayer surface. The difficulty in achieving such a PAES conformation explains the low nanotube grafting density. To overcome this difficulty, an excess of PAA was reacted with APTMS-modified mica and amino-functionalized nanotubes were then reacted with the grafted PAA chains. Figure 4 shows two AFM images of a mica plate after nanotube grafting. The grafting density is now much higher. While standing nanotubes were found predominantly in most AFM images such as the one shown in the 3D image on the right, lying and slanting nanotubes are seen still in certain images such as the one shown in the left 2D image of Figure 4.

Water Contact Angles. Despite the low grafting density, water contact angle on a nanotube-grafted glass plate using succinic anhydride as the spacer was high at $(90 \pm 1)°$ as shown in Figure 2. This represents a substantial increase from $(19 \pm 2)°$ for the succinic-acid-covered surfaces and is even higher than $(82 \pm 2)°$ measured on a flat PS plate. Thus, this suggests a dramatic topographic effect of the nanotubes in modifying surface properties.[38]

Despite the higher nanotube grafting density, the θ_W value on nanotube-grafted surfaces using PAA as the connector was low at $68 \pm 3°$. This apparent controversy had its roots most likely in the standing position adopted by most nanotubes in this case. With standing nanotubes, the water droplets may rest on the polar terminal amino groups.

Nanotube Grafting Using Suberic Acid as the Connector. In the above-discussed cases we created carboxyl-group-modified surfaces in one step, and the surface carboxyl groups were reacted with PAES-terminated nanotubes to graft the nanotubes in a subsequent step. A molecule containing two or more carboxyl groups can be used to couple APTMS-modified

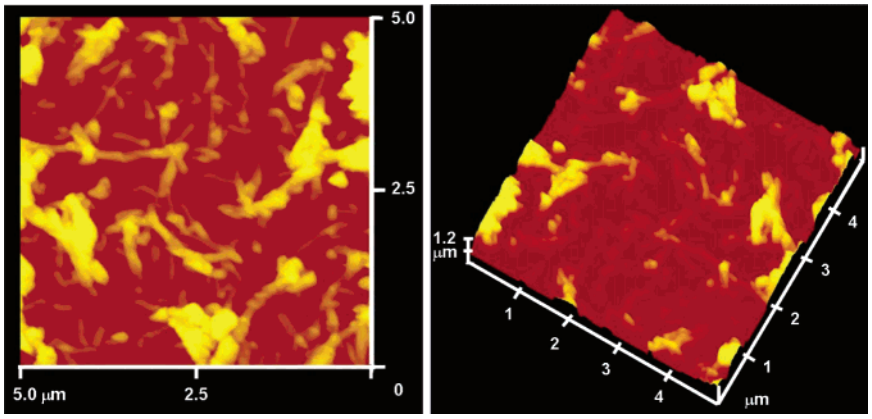

Figure 5. AFM images of nanotubes grafted on mica surface using suberic acid as the connector.

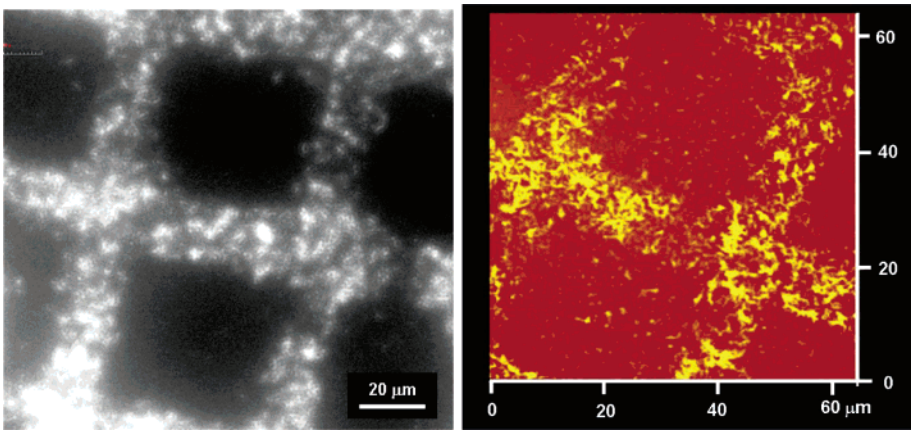

Figure 6. Fluorescence microscopic (left) and AFM (right) images of the glass surface after grafting of nanotubes onto a patterned surface.

Scheme 2. Processes Involved for Patterned Grafting of Nanotubes

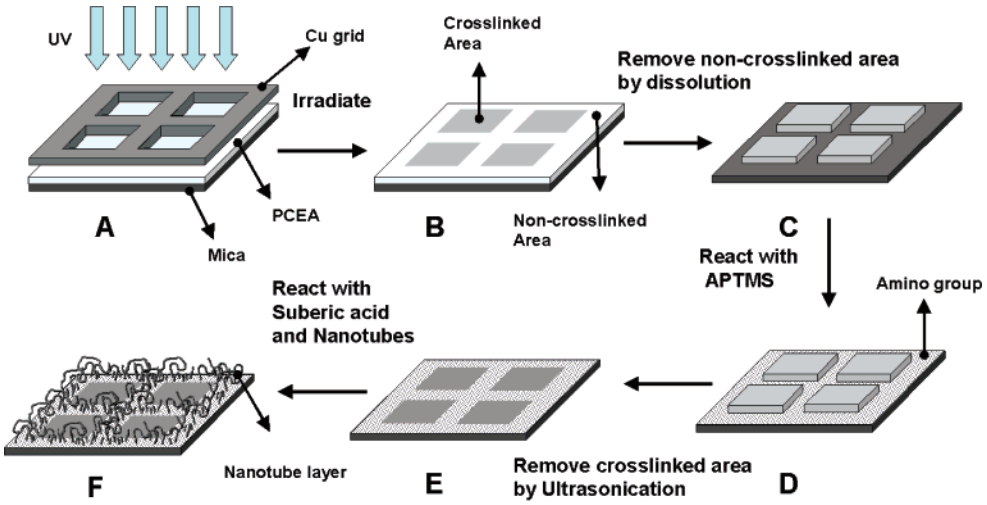

mica and PAES-PS-PAES-modified nanotubes also using a one-pot strategy. Such a strategy is simpler but should lead to a mixture of products because suberic acid can also couple different nanotubes. We decided to try this approach as we thought that the uncontrolled coupling could increase the surface roughness. Figure 5 shows two AFM images of nanotubes grafted on mica using suberic acid as the connector. The lying tubes can now reach heights exceeding 600 nm suggesting extensive inter-tube linking and nanotube piling. More interestingly, the θ_W value is now (101 ± 4)°, which is larger than (90 ± 1)° on surfaces using succinic anhydride as the connector in agreement with the increased surface roughness effect.

Patterned Grafting of Nanotubes. Our strategy for achieving patterned grafting of nanotubes is illustrated in Scheme 2. To obtain a glass plate with a chemically patterned surface, we started by spin-casting a PCEA film. The film was irradiated using a TEM grid as the mask to cross-link PCEA in the grid square regions (A → B). PCEA in the unexposed TEM grid bar regions was rinsed off by ultrasonication in chloroform for 2.5 h (B → C). We then exposed the patterned plates to APTMS

and DPEA (*N*,*N*-diisopropylethylamine, C → D). After APTMS treatment, the cross-linked PCEA regions were mostly removed by ultasonication in chloroform for another 3.5 h (D → E). Amino-patterned surfaces were then reacted with nanotubes using suberic acid as the connector (E → F) to yield finally nanotube-patterned surfaces. Suberic acid rather than PAA or succinic anhydride was used mainly for experimental simplicity. Except steps A → B and C → D, our success in achieving the other steps has been confirmed by AFM and/or fluorescence microscopy.

Figure 6 shows a fluorescence microscopic image of a nanotube-patterned glass surface. The fluorescent nanotubes are expectantly concentrated in the original TEM grid bar regions which were not irradiated during the PCEA film photolysis step. Such a conclusion is confirmed also by AFM experiments with an image shown in Figure 6. Aside from confirmation of nanotube concentration in the grid "bar" regions, we notice the presence of some nanotubes in the mesh square regions as well. This was possible because a cross-linked PCEA film was partially permeable to APTMS and DPEA under our experimental conditions. We did not attempt further optimization of reaction times between APTMS and mica surfaces because the selective grafting of the nanotubes in the grid bar regions is unambiguously evident here already.

III. Conclusions

Mica or glass plates with surface amino groups were prepared by exposing such plates to APTMS and DPEA. Such amino groups were then converted to carboxyl groups via reaction with succinic anhydride or PAA. The PAA core chains of PS-PCEMA-PAA nanotubes could be used not only for the introduction of terminal functional amino groups but also for the introduction of fluorescent dyes such a fluoresceinamine. Such nanotubes bearing terminal amino groups could be attached covalently to mica or glass plates bearing surface carboxyl groups. When PAA was used as the connector between the nanotubes and APTMS-modified mica or glass surfaces, the nanotube grafting density was high. Most of the grafted nanotubes remained standing even after solvent evaporation. Suberic acid could be used to couple nanotubes and APTMS-modified mica or glass surfaces in a one-pot process. The nanotube-grafted surfaces in the last case were rugged and not well-defined probably for the concurrent coupling of different nanotubes during the tube grafting process. Water contact angle on such surfaces was substantially larger than that on PS plates despite the incomplete surface coverage by nanotubes. Reacting nanotubes bearing terminal amino groups with carboxyl-patterned surfaces allowed patterned grafting of the nanotubes.

Acknowledgment. The Special Research Opportunity Program of the Natural Sciences and Engineering Research Council of Canada is gratefully acknowledged for sponsoring this research. G.L. thanks the Canada Research Chairs program for a Research Chair position in Materials Science. The Canada Foundation for Innovations and the Ontario Innovation Trust are acknowledged for an infrastructure grant to purchase the atomic force and fluorescence microscope.

Supporting Information Available: Experimental details for measurement techniques, nanotube synthesis and derivatization, surface modification, surface patterning, and nanotube grafting are available free of charge via the Internet at http://pubs.acs.org.

JA066684D